Supplementary Information (SI) for Nanoscale.
This journal is © The Royal Society of Chemistry 2026

Supplementary information

Nanocomposite Hydrogels with Temperature-Accelerated Antioxidant Activity for Ocular Applications

Hyeonah Lee[a], Serim Byun[a], and Hyeran Noh*[a,b]

a Department of Optometry, Seoul National University of Science and Technology, 232 Gongneung-ro, Nowon-gu, Seoul 01811, Korea

b SeoulTech-KIRAMS Graduate School of Biomedical Science and Engineering, Seoul National University of Science and Technology, Seoul 01811, South Korea

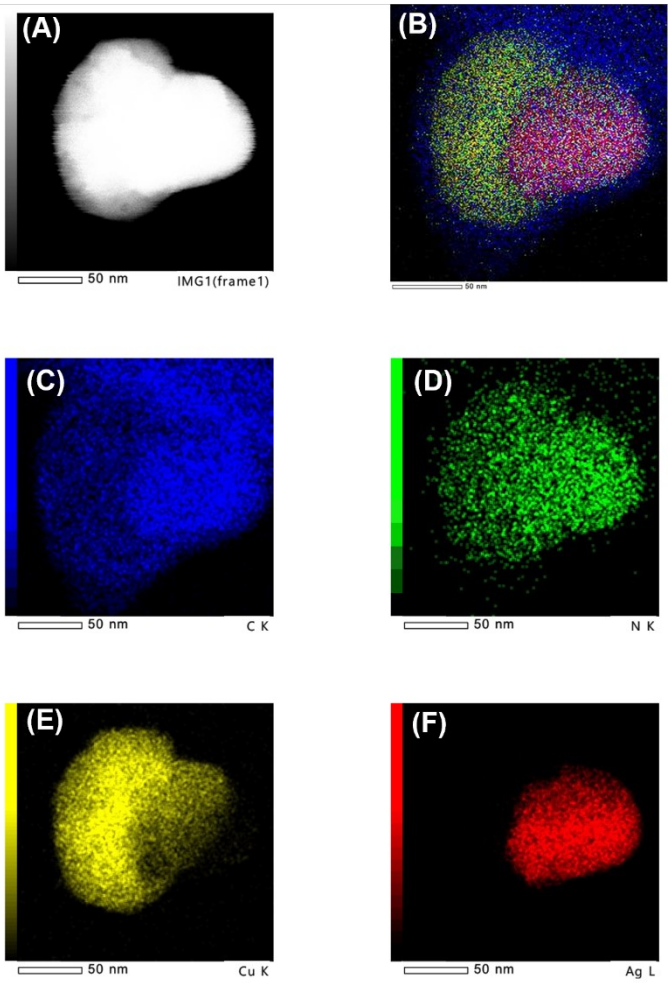

Fig. S1 HAADF-STEM image and corresponding EDS elemental mapping of the pNIPAM–Ag/Cu@Cu nanocomposite. (A, B) HAADF-STEM images. (C) C K map and (D) N K map, both originating from the pNIPAM polymer matrix. (E) Cu K map showing Cu distribution across the entire nanoparticle volume. (F) Ag L map showing Ag confined to the central core region, confirming preservation of the Ag core / Cu shell architecture within the pNIPAM matrix. Scale bars, 50 nm.

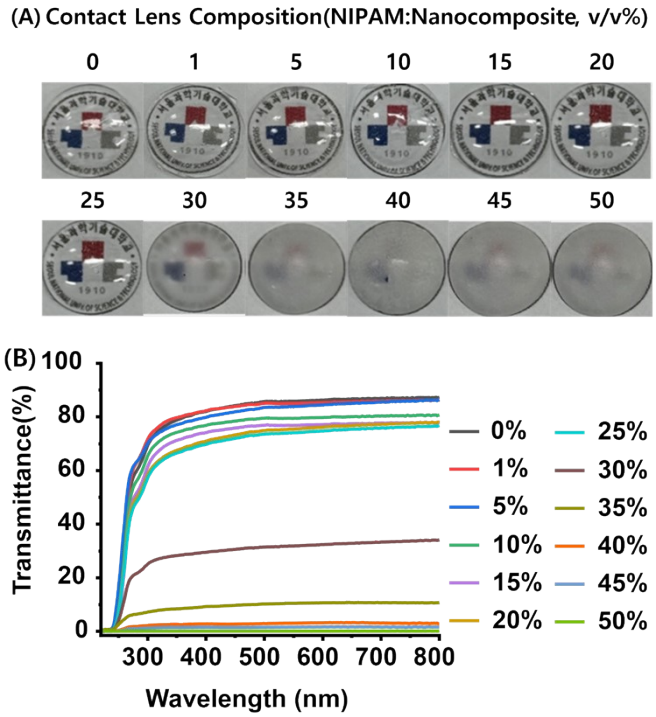

Fig. S2 Optical properties of nanocomposite contact lenses as a function of nanoparticle concentration. (A) Digital photographs showing the visual clarity of lenses formulated with varying concentrations (v/v%) of the nanocomposite, (B) UV–Vis transmittance spectra of the lenses.

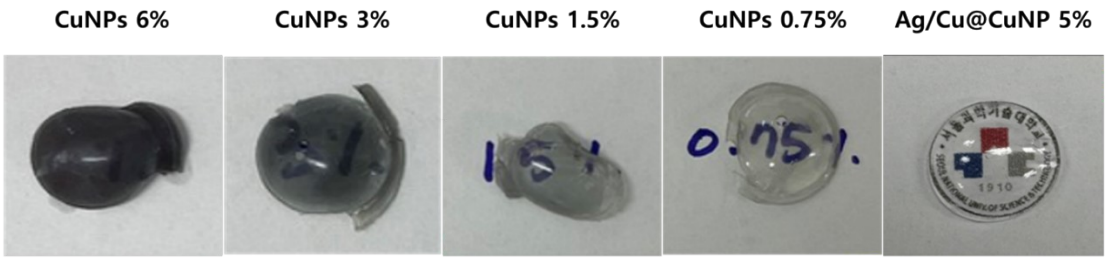

Fig. S3 Photographic images of hydrogel contact lenses containing only Ag/Cu@Cu bimetallic nanoparticles at various loadings (0.75%, 1.5%, 3%, and 6% v/v). Transparency decreased progressively with increasing nanoparticle content, with the highest loading (6%) exhibiting pronounced whiteness and opacity. These findings highlight that, in the absence of pNIPAM encapsulation, Ag/Cu@Cu nanoparticles induce strong light scattering and substantially compromise lens optical performance.

Table S1. Comparative summary of representative antioxidant strategies for ocular applications.

System	Transmittance	Stability	Temp. Response	Mechanism	Ref.
Conventional antioxidant-incorporated ocular systems	Decreases with agent release; transparency loss over time	Poor; continuous passive release depletes agent; low bioavailability	None (passive diffusion)	Non-enzymatic, consumable (e.g., Vit. C/E)	[10, 11, 18]
Enzyme-mimetic nanoparticle (nanozyme) systems	Compromised at high NP loadings due to scattering	Moderate; NP aggregation without stabilizing matrix	None	Enzymatic SOD/CAT-mimetic	[28, 30, 33]
Unencapsulated NP-loaded hydrogels	Reduced at high loadings due to aggregation	Poor; oxidation-driven degradation within hours	None	Surface redox (non-enzymatic)	[19, 20, 36]
pNIPAM–Ag/Cu@Cu (This work)	**>70% at ≤25% v/v loading; visually clear**	**High; >24 h sustained activity; pNIPAM encapsulation**	**Yes; LCST-mediated (k doubles, 25→35 °C)**	**Dual: SOD-mimetic + non-enzymatic (Ag/Cu synergy)**	**This work**

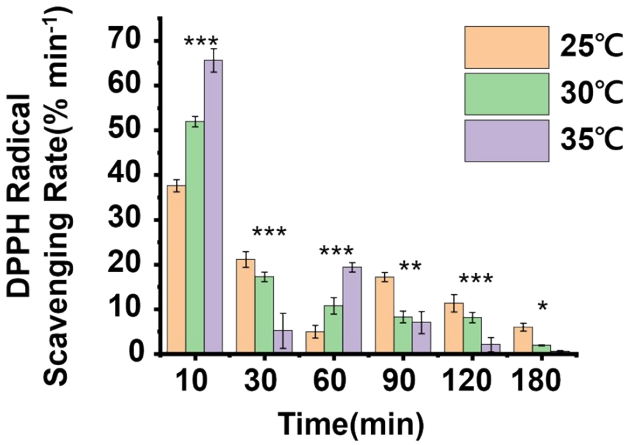

Fig. S4 Thermoresponsive antioxidant activity of the nanocomposite contact lenses (20% v/v).; Instantaneous scavenging rates (%/min) calculated over discrete time intervals. Asterisks indicate statistical significance between temperature groups at each time interval, as determined by post-hoc tests (*$p < 0.05$, **$p < 0.01$, ***$p < 0.001$). Data are presented as mean ± SD (n = 5 per group).

Table S2. Linear regression statistics for pseudo-first-order kinetic fits of DPPH radical scavenging at each temperature.

Temperature (°C)	Temperature (K)	Rate constant k (%/min)	ln(k)	R^2	n
25	298.15	0.37	−0.994	0.949	5
30	303.15	0.58	−0.545	0.959	5
35	**308.15**	**0.74**	**−0.301**	**0.962**	**5**

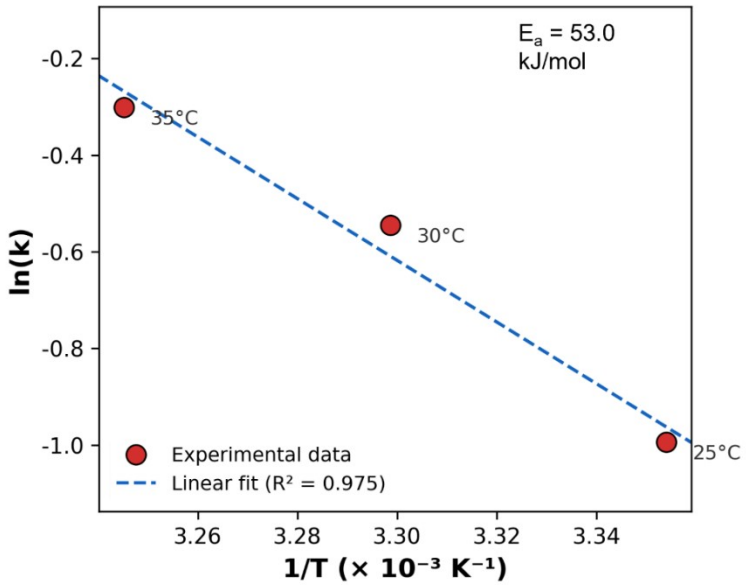

Fig. S5 Arrhenius plot of the temperature-dependent rate constants for DPPH radical scavenging by pNIPAM–Ag/Cu@Cu nanocomposite contact lenses (20% v/v).

Table S3. Two-way ANOVA results for DPPH radical scavenging by nanocomposite contact lenses.

Source of Variation	**df**	**p-value**	**Significance**
Time (main effect)	5	$p < 0.0001$	***
Temperature (main effect)	2	$p = 0.583$	n.s.
Temperature × Time (interaction)	10	$p < 0.0001$	***
Residual (within-group)	72	—	—